Dynamic Inter-Cell Interference Coordination to Optimize XR and eMBB Coexistence

Paymard, Pouria; Amiri, Abolfazl; Kolding, Troels E.; Pedersen, Klaus I.

Published in:
2024 IEEE 100th Vehicular Technology Conference, VTC 2024-Fall - Proceedings

DOI (link to publication from Publisher):
10.1109/VTC2024-Fall63153.2024.10757991

Publication date:
2024

Document Version
Accepted author manuscript, peer reviewed version

Dynamic Inter-Cell Interference Coordination to Optimize XR and eMBB Coexistence

Pouria Paymard[1], Abolfazl Amiri[2], Troels E. Kolding[2], and Klaus I. Pedersen[1, 2]

[1]Department of Electronic Systems, Aalborg University, Aalborg, Denmark
[2]Nokia, Aalborg, Denmark

***Abstract*—This paper presents a dynamic inter-cell interference coordination (ICIC) technique that enhances extended reality (XR) capacity while minimizing the impact on enhanced mobile broadband (eMBB) traffic in a multi-cell multi-user network. The network identifies victim XR users based on their performance metrics and dynamically coordinates with aggressor cells for muting in specific transmission time intervals to alleviate interference for the victim users. Extensive dynamic system-level simulations demonstrate the effectiveness of the proposed ICIC scheme, achieving a 22-32% enhancement in XR capacity while incurring a degradation of 12-22% in average eMBB cell throughput.**

I. Introduction

The emergence of immersive technologies like extended reality (XR) has triggered research for its improved support in fifth-generation (5G)-Advanced networks and beyond [1]–[3]. XR applications demand high data rates, low latency, and high reliability to deliver seamless, immersive experiences. For instance, streaming high-definition XR videos requires data rates of tens of megabits per second (Mbps). Additionally, XR applications necessitate low latency, typically between 10 and 30 milliseconds (ms), to maintain the illusion of a physical presence in the virtual world [1]. Furthermore, high reliability is crucial to ensure that users do not experience unexpected interruptions or glitches during their immersive experiences. These stringent requirements pose significant challenges to existing cellular networks, calling for fundamental enhancements to meet the demands of immersive technologies.

Extensive research efforts have been dedicated to XR traffic handling over wireless networks in both academia and industry [4]–[6]. The 3rd Generation Partnership Project (3GPP) Release-18 technical report introduced several XR-related enhancements to radio resource management (RRM), including XR-optimized configured grant, enhanced buffer status report (BSR), a new refined BSR table to suit XR traffic, and XR application awareness to gNB [2]. The 3GPP Release-19 work item considers the handling of multiple quality of service (QoS) flows and QoS inter-dependencies of XR traffic, as well as enhanced delay-aware packet scheduling, to effectively manage XR traffic [3].

One of the primary objectives of 5G networks and beyond is to seamlessly support a diverse range of services, including enhanced mobile broadband (eMBB) and XR. Enhancing capacity for XR traffic needs to be balanced with the co-existence of existing traffic types, like eMBB. This highlights the importance of RRM to ensure optimal performance across the network. With user scheduling prioritization, high-priority services such as XR first get served, followed by eMBB transmissions [7]. The ability to support XR and eMBB traffic, does, however, heavily depend on the inter-cell interference (ICI) in the network.

Numerous ICI Coordination (ICIC) techniques have been developed to mitigate ICI of orthogonal frequency division multiple access (OFDMA)-based systems [8]–[10]. The authors in [8] first address various interference issues in both uplink and downlink and then introduce diverse solutions for interference management in 5G New Radio networks. including inter-cell rank coordination with advanced interference-aware receivers [11]. Additionally, another approach proposed in [12] utilizes on-demand power boosting and inter-cell coordination to meet the stringent requirements of critical data without compromising overall spectral efficiency. This approach involves boosting the power of the time-frequency resources allocated to victim user equipment (UE) while temporarily silencing the aggressor cell to minimize interference. Another effective ICIC technique specifically addresses interference in heterogeneous networks and introduces the almost blank subframes approach, during which the aggressor macro cell temporarily stops the data transmission, allowing co-channel deployed pico cells to serve distant UEs that would otherwise suffer from high macro cell interference [13]. The study in [14] on the performance of 5G-Advanced networks with mixed XR and eMBB traffic revealed that imposing resource restrictions on eMBB transmissions has promising performance benefits, although not proposing detailed dynamic solutions. One candidate solution to enable better handling of XR and eMBB traffic is, therefore, QoS-aware techniques.

The key challenge is how to practically realize QoS-aware ICIC schemes that can boost the overall network XR performance, while ensuring that eMBB performance is only minimally impacted. This paper addresses this challenge by proposing a dynamic ICIC technique tailored for the coexistence of XR and eMBB traffic in 5G-Advanced networks. The contributions of this paper are outlined as follows:

- We introduce a new proactive time-domain, QoS-aware, dynamic ICIC technique to manage interference in the network with both XR and eMBB users. Thereby, the next

generation NodeB (gNB) identifies its XR UEs highly impacted by ICI (victim UEs) based on their performance and then coordinates with the dominant interfering cells (aggressor cells) to temporarily silence their transmissions during specific transmission time intervals (TTIs).
- The performance of the proposed ICIC technique is assessed through system-level simulations conducted in indoor hotspot (InH) network deployment, which is known to be a challenging interference-limited scenario. System-level simulation results demonstrate that the proposed scheme effectively enhances XR capacity while minimizing the impact on average eMBB cell throughput.

II. Setting the Scene

A. Traffic Model

For the XR traffic, we adopt the widely accepted downlink XR traffic model in [1] where the XR application server generates XR video frames at a fixed interval of 16.67 ms. These frames experience random delay jitter, distributed according to a truncated Gaussian distribution with a mean of zero and a variance of ± 4 ms. Two typical XR source data rates (SDRs) of 30 and 45 Mbps are assumed. The size of XR video frames also follows a truncated Gaussian distribution. Consequently, the average generated packet size (in Kbits) can be calculated as $L = \text{SDR(Mbps)} \times 16.67\text{(ms)}$, with a standard deviation of 10.5% of L. The size of XR video frames is truncated between 50% and 150% of L.

For the eMBB traffic, we assume a simple best-effort full-buffer model, implying that there is always infinite eMBB load at the gNB, ready to be transmitted to eMBB UEs upon receiving an allocation.

B. Deployment Model

The study adopts an InH deployment scenario, specified in [1]. This configuration features low-power small cells densely deployed to cover an area of $120 \times 50\,\text{m}^2$. There are $B = 12$ ceiling-mounted gNBs, arranged in two rows of 6 gNBs with an inter-site distance of 20 meters. UEs are assumed to be uniformly distributed in the network layout with 100% indoor placements and semi-stationary positions [1]. To include small-scale radio propagation effects, the UE speed is set to 3 km/h. Each cell in the network serves an equal number of UEs. The number of eMBB UEs is set to 5 UEs per cell with full-buffer traffic, while the number of XR UEs varies as specified for each simulation.

C. 5G New Radio Frame Structure

We focus on the downlink transmissions in an OFDMA system operating in time division duplex (TDD) mode. We employ a DDDSU duplexing pattern, where D, S, and U represent downlink, special, and uplink slots, respectively. All the slots comprise 14 symbols. The special slot is configured with a 10 downlink symbols, a 2-symbol guard period, and 2 uplink symbols. We set a sub-carrier spacing of 30 kHz and a carrier bandwidth of 100 MHz. Each physical resource block (PRB) is composed of 12 sub-carriers, resulting in 272 PRBs. The sub-carrier spacing setting leads to a TTI of 0.5 ms.

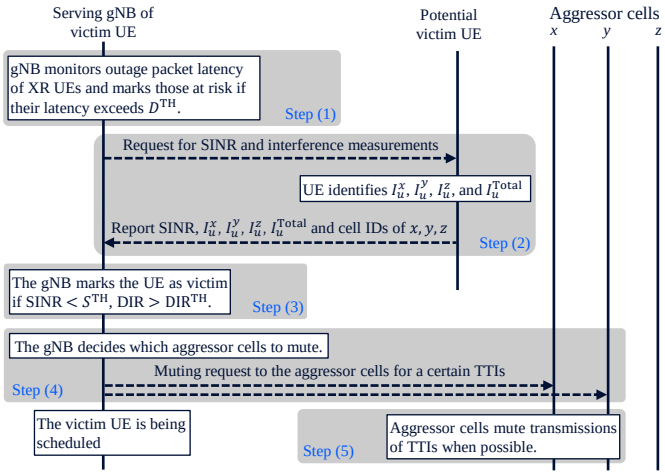

Fig. 1. Signaling flow diagram illustrating the proposed procedure.

D. Basic Packet Scheduling and Link Adaptation

Each transport block (TB) is composed of code block groups (CBGs) to enhance the resource efficiency in hybrid automatic repeat request (HARQ) retransmissions. Dynamic link adaptation is assumed. Enhanced CQI feedback is used to control the number of failed CBGs during initial transmissions [15]. Multi-bit HARQ feedback is sent to the gNB, indicating which CBGs failed. An outer loop link adaptation (OLLA) algorithm utilizes this feedback to control the CBG error rate [16].

Basic radio resource scheduling is performed as per modified largest weighted delay first (M-LWDF) policy [17]. HARQ retransmissions are prioritized over first transmissions. For each TTI, candidate UEs are ordered based on QoS class, and accordingly, the available PRBs are first allocated to XR UEs and then to eMBB UEs. The allocation process continues until either all PRBs are occupied or all UEs in the queue have been scheduled.

E. Key Performance Indicators (KPIs)

The primary KPIs are the XR satisfaction ratio and XR capacity, as defined in the 3GPP evaluation methodology [1], [2]. XR satisfaction ratio measures the percentage of XR UEs that receive at least 99% of their XR video frames within the specified packet delay budget (PDB). XR capacity is the maximum number of XR UEs supported per cell while maintaining a satisfaction ratio of at least 90%. Additionally, we examine other KPIs such as experienced signal-to-interference-plus-noise ratio (SINR), experienced delay, average muting ratio, and average eMBB cell throughput.

III. Proposed Dynamic ICIC Technique and RRM

The design principle as well as algorithm implementation are explained as follows aided by Fig. 1. We assume a

distributed proactive ICIC scheme that runs in each gNB. The serving cell monitors the QoS for its served XR users, and when the QoS requirements for a UE are about to be violated (e.g., PDB is very close to expiry), actions are taken to determine if the situation can be improved via ICIC actions. To do this, the serving cell requests SINR and interference measurements from the XR UE, which experiences low QoS, and uses those to determine if the ICI is the cause of the problems. When this is the case, the gNB determines which cell, or cells, are causing the ICI problem (denotes the aggressor cell, or aggressor cells). If the XR user in question is found to be an ICI victim UE, its corresponding aggressor cell(s) is then asked to mute its (or their) transmission resources of lower priority UEs at the times when the victim UE will be scheduled. Muting means that the aggressor cell will not schedule transmissions of any eMBB UEs and XR UEs with robust QoS conditions at the TTIs when the victim UE is scheduled by its serving cell. The individual steps of the proposed ICIC scheme are explained in greater detail in the following:

Step 1) Each gNB continuously monitors the performance of its XR UEs. If an XR UE u is found to be close to its minimum QoS requirement, it is subject to further investigation. As the primary QoS requirement for the XR users is the 99-percentile of the experienced XR frame delay, the gNB monitors if the 99-percentile of the UE's experienced frame delay exceeds a predefined delay threshold, D^{TH}. We assume $D^{\text{TH}} = 0.9\times$ PDB, given the assumed XR KPI and traffic model.

Step 2) For the XR UEs that are found to be close to their minimum QoS requirements, it is evaluated if this is caused by ICI problems. This is done by requesting SINR and interference measurements of the subject matter XR UE. The rationale for this is that UEs with low SINR and high dominant interference ratio (DIR) are more likely to be suffering from ICI. This comes from [18], where it was shown that the SINR improvement from such muting is proportional to the DIR. Hence, if an XR UE with lower experienced QoS and an average SINR below S^{TH} and DIR above DIR^{TH}, it is labeled as a victim UE, triggering ICIC actions in an attempt to improve its performance. Each victim XR UE is instructed by its serving gNB to gather information about the Interference of its top-aggressor cells and their corresponding cell IDs. To accomplish this, UE u performs reference signals received power (RSRP) measurements to assess the received RSRP from neighboring cells, $I_u^k,\ \forall k \in \{1, \cdots, B\}$. The UE u reports the average experience SINR, the top three strongest RSRP cell measurements ($I_u^x > I_u^y > I_u^z$), and their corresponding cell IDs (x, y, z) together with the total received interference ($I_u^{\text{Total}} = \sum_{\forall k} I_u^k$).

Step 3) The gNB serving the victim UE calculates the DIR of UE u using the following expression [18]:

$$\text{DIR}_u^x = \frac{I_u^x}{I_u^{\text{Total}} - I_u^x + N_u}, \tag{1}$$

where I_u^x is the interference from the first dominant interferer cell x for UE u, and N_u is the background noise. Given the information provided by the UE, the gNB can estimate if muting the dominant aggressor cell(s) is sufficient to bring the SINR above S^{TH}, since the SINR improvement from such muting is proportional to the DIR [18]. If that is not the case, the second or third strongest aggressor cells are also muted until the SINR is estimated to be above S^{TH}. The DIR of the top two aggressors is expressed as follows:

$$\text{DIR}_u^{x,y} = \frac{I_u^x + I_u^y}{I_u^{\text{Total}} - I_u^x - I_u^y + N_u}, \tag{2}$$

where I_u^y is the interference from the second dominant interfering cell y for UE u. Similarly, the DIR of the top three aggressors is expressed as follows:

$$\text{DIR}_u^{x,y,z} = \frac{I_u^x + I_u^y + I_u^z}{I_u^{\text{Total}} - I_u^x - I_u^y - I_u^z + N_u}, \tag{3}$$

where I_u^z is the interference from the third strongest dominant interferer cell z for UE u.

Step 4) When the gNB has identified one, or more, of its XR UEs as victims, it informs the aggressor cell(s) to mute at the times when the victim UE will be scheduled. For the current XR traffic model, where the XR frame arrives every 16.66 ms on average, and typically requires 2-4 TTIs for scheduling (including potential HARQ retransmissions), this means muting of only 2-4 TTIs for every 33 TTIs. Conveying such information to the aggressor cell happens via the Xn inter-gNB interface, using the Xn application protocol [19].

Step 5) The aggressor cell receiving the muting request will thereafter avoid scheduling eMBB UEs and XR UEs with a head-of-line (HoL) packet delay below a predefined threshold (equivalent to 10% of the PDB) during the TTIs where the other-cell victim XR UE(s) will be scheduled However, the aggressor cell is still allowed to schedule its own critical XR UEs as needed to fulfill its QoS target if colliding with the muting requests.

IV. Simulation Methodology

The proposed ICIC technique is evaluated through comprehensive dynamic system-level simulations in line with the system model in Section II. The simulator is developed based on 5G New Radio evaluation methodology assumptions for XR Release-18 [1], [2]. It incorporates detailed modeling of RAN user plane protocols, RRM mechanisms, 3D radio propagation, and traffic models frequently employed in the 3GPP evaluation methodology. Table I summarizes the key system parameters and assumptions. The simulation methodology, and simulation tool, are the same as used in the previous studies in [20].

At the start of each simulation, a fixed number of XR and eMBB users are randomly placed within the simulated InH scenario, with an equal number of XR and eMBB users per cell. After the creation of the environment, the simulation is started. It runs on the resolution of orthogonal frequency division multiplexing (OFDM) symbols (time-domain) and sub-carrier (frequency-domain). Each simulation starts with a so-called warm-up phase aimed at stabilizing all control loops for link adaptation, MIMO adaptation, scheduling, etc. In this

study, we also use the warm-up time to identify potential victim XR UEs as per the criteria outlined in Section III. The simulation continues after the warm-up time, where potential muting to protect the identified victim XR UEs is carried out. For the sake of simplicity, the corresponding inter-gNB signaling of messages to request muting is assumed to happen instantly with zero latency and no errors. Each scheduled transmission from the gNBs occurs according to the scheduling policy, involving potential HARQ retransmissions, dynamic link adaptation, MIMO adaptation, etc. The decoding of each transmission is modeled via the standard link-2-system level interface based on the mean mutual information per coded bit (MMIB) scheme [21]. Note that transmissions with CBGs, and CBG-based HARQ feedback, are assumed as outlined in Section II-D.

The simulation length after the warm-up phase is set to be sufficiently long to be able to extract reliable statistics for the main KPIs. This is done by setting the simulation length, so it corresponds to at least 600 XR frame transmissions from each XR UE. This allows us to estimate, with 95% confidence, whether $99\% \pm 1\%$ of the frames are successfully received for each XR UE within the PDB (i.e. in line with the XR satisfaction criteria). As each simulation involves N XR UEs per cell and C cells, this results in XR statistics from $C \times N$ XR UEs per simulation run. To ensure that we sample different spatial placements of UEs, we repeat M independent simulation runs – each with a new random placement of UEs. This means that each simulation campaign includes $C \times N \times M$ XR UEs. Therefore, when $N = 7, C = 12$, and $M = 12$, we have "XR satisfaction statistics" from 1008 XR UEs, which is sufficient to reliably determine if 90% of the XR UEs are satisfied in line with the XR capacity definition.

For more background information on the conducted simulations, see the tutorial on 5G-Advanced system-level simulations in [22].

V. Performance Results

A. Setting the parameters of the ICIC algorithm

As described in Section III, the proposed ICIC solution includes latency, SINR, and DIR threshold parameters to determine if an XR UE is a victim of ICI that shall trigger ICIC actions in the network. The setting of these parameters is therefore important. Given the assumed XR traffic model and PDB of 10 ms, we set the latency threshold to $D^{\text{TH}} = 9$ ms ($0.9\times$ PDB) to mark when a UE is getting close to the limits of its QoS target. The setting of the SINR threshold, S^{TH}, can be roughly calculated if assuming that the gNB can transmit one XR frame over X slots on the full carrier bandwidth. Within the PDB of 10 ms, the assumed radio frame structure has 15 downlink TTIs. If those must be shared by 7 XR UEs (which can typically be supported in a cell) it means $X = 2$. With the assumed average XR frame size of 500 kbits and 100 MHz bandwidth, it means that the required MCS is 64QAM and a code rate of 0.873. This MCS approximately requires a SINR of 18 dB.

TABLE I
Summary of System-Level Evaluation Parameters

Parameter	Setting
Deployment (Area)	InH (120m × 50m)
Layout	12 cells
Inter-site Distance	20 m
gNB height	3 m
gNB Tx power	31 dBm
Control channel overhead	1 OFDM symbol
Bandwidth	100 MHz
Sub-carrier spacing	30 kHz
MIMO scheme	SU-MIMO with rank adaptation
Modulation	QPSK to 256QAM
gNB Tx processing delay	2.75 OFDM symbols
gNB antenna	1 panel with 32 elements (4 x 4 and 2 polarization)
UE speed	3 km/h
UE height	1.5 m
UE Rx processing delay	6 OFDM symbols
UE receiver	MMSE-IRC
Number of UE antennas	2 dual-polarized Rx antennas
eMBB Traffic	5 eMBB UE/cell with full-buffer
XR Traffic model	quasi-periodic with truncated Gaussian
XR frame rate	60 fps
Average frame size (30 Mbps)	62 kB
Average frame size (45 Mbps)	93 kB
HARQ scheme	CBG-based HARQ retransmissions
CQI	Periodic CQI every 2.5 ms
Target CBG error probability	2 out 8 CBGs

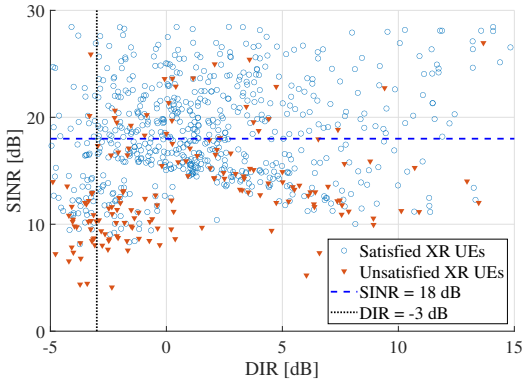

Fig. 2. The average SINR versus the DIR experienced by XR UEs when there are 7 connected XR UEs per cell and the average XR SDR of each UE is 30 Mbps.

To determine the proper ICIC parameter settings, Fig. 2 shows a scatter plot of XR UEs average SINR and DIR for a simulation without ICIC with 7 XR UEs per cell. The scatter plot shows whether the UEs are satisfied (i.e., successfully received at least 99% of their XR frames within the PDB), or not. As observed in Fig. 2, unsatisfied XR UEs are spread across different SINR values, with a higher density below 18 dB. For unsatisfied XR UEs exceeding this threshold, ICIC offers minimal benefit as those UEs reside in congested cells where ICI is not the primary concern. We also observe that a DIR^{TH} of -3 dB, which corresponds to approximately 2 dB SINR gain if eliminating the dominant interferer [18], appears to be a good setting.

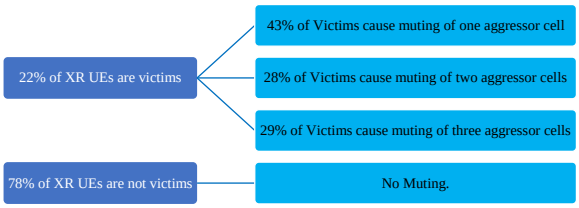

Fig. 3. Percentage of victim UEs, and percentage of number of aggressor cells requested to be muted.

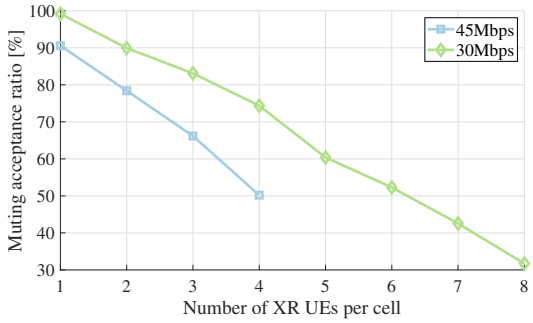

Fig. 4. Muting acceptance ratio of the proposed ICIC versus the number of connected XR UEs per cell for different XR SDRs.

B. Muting Statistics

Given the aforementioned parameter settings for labelling XR UEs as victims, Fig. 3 shows the percentage of XR victim UEs in the network, as well as statistics for how many aggressor cells they trigger muting requests for. We observe that 22% of XR UEs are marked as victims. Among the victim UEs, 43% of those causes request muting of only their top aggressor cell, while 28% of the victim UEs trigger muting requests for two aggressor cells. The remaining 29% of the victim UEs trigger requesting muting of three aggressor cells to mitigate the experienced ICI and meet the UEs' minimum SINR requirements.

Fig. 4 illustrates the muting acceptance ratio across the network for different SDRs and the number of connected XR UEs per cell. The muting acceptance ratio is defined as the proportion of muting requests where the receiving cell indeed mutes (and refrains from scheduling any of its own XR/eMBB UEs) out of all muting requests. In low load scenarios, e.g., 2 XR UEs per cell, approximately 90% and 80% of muting requests are accepted by aggressors in the SDRs 30 Mbps and 45 Mbps, respectively. As the number of XR UEs increases within the network, the number of XR victims also grows. This growth leads to both more muting requests and higher probabilities of aggressor cells being requested to mute. As a result, they will have to prioritize the scheduling of their own XR UEs, which means they may not fulfill all muting requests. For example, when the XR load reaches 7 UEs per cell, the muting acceptance ratio declines to 43%.

Fig. 5 shows the resulting average muting ratio across the network versus the number of connected XR UEs per cell. The

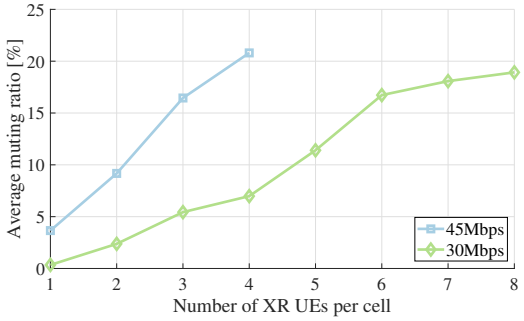

Fig. 5. Average muting ratio of the proposed ICIC versus the number of connected XR UEs per cell for different XR SDRs.

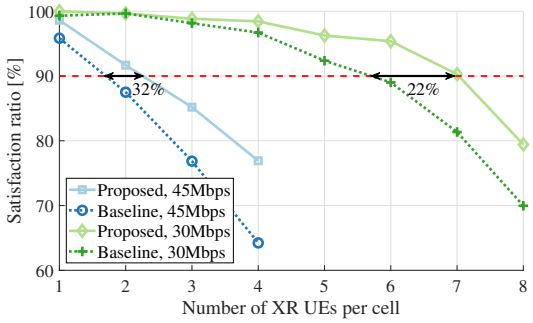

Fig. 6. XR Satisfaction ratio versus number of connected XR UEs per cell for three different schedulers.

muting ratio increases with increasing XR UE density in the cells. For example, the average muting ratio in the network is 14% for the 45 Mbps at 3 XR UEs/cell and is 16% for the 30 Mbps at 7 XR UEs/cell. One key observation here is that a muted aggressor cell not only improves the SINR of the victim UEs but also the SINR of all the surrounding UEs. This eventually helps boosting the performance of both XR and eMBB UEs in the entire system.

C. The impact of dynamic ICIC on the XR performance

To assess the capacity gain of the proposed ICIC technique, we evaluated the XR satisfaction ratio for two XR SDRs of 30 Mbps and 45 Mbps in Fig. 6. As expected, the XR satisfaction ratio declines with increasing number of XR UEs per cell. The results demonstrate that the proposed ICIC technique consistently enhances the XR satisfaction ratio for both XR SDRs. For the 30 Mbps case, a 22% increase in XR capacity at the 90% satisfaction ratio target is observed from the proposed ICIC scheme (i.e., the XR capacity is increased from 5.7 UEs/cell to 7 UEs/cell). This improvement comes from the effective muting of aggressor cells to protect victim UEs suffering from ICI.

Fig. 7 presents the empirical cumulative distribution function (eCDF) of post-detection SINR experienced by victim UEs without ICIC (baseline) and after ICIC is applied. The results indicate a significant SINR improvement for the victim XR UEs as a result of the proposed ICIC technique compared

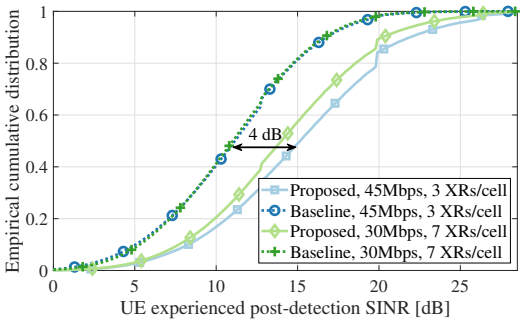

Fig. 7. The eCDF of experienced SINR for XR victim UEs.

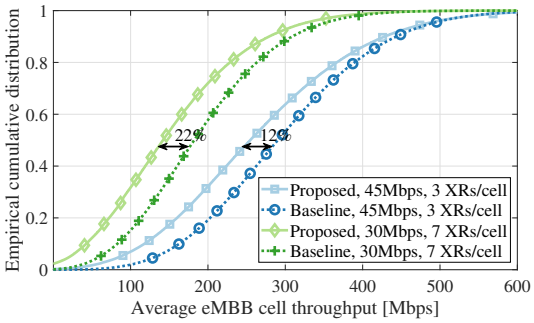

Fig. 8. eCDF of average eMBB cell throughput for different XR SDRs.

to the baseline. The median SINR gain for the 45 Mbps SDR is about 4 dB. This improvement stems from the muting of aggressor cells, thereby reducing interference for victim UEs.

D. The impact of dynamic ICIC on the eMBB performance

Fig. 8 depicts the eCDF of the average eMBB cell throughput for 30-45 Mbps XR SDRs. Per-UE throughput samples are collected and then averaged across each cell for this CDF plot. As a general trend, the eMBB cell throughput for the 30 Mbps with 7 XR UEs/cell is lower than the case with three 45 Mbps XR UEs/cell due to the allocation of fewer PRBs to eMBB UEs. While there is a reduction in eMBB cell throughput when the proposed ICIC technique is applied, the decrease is substantially less than the gain achieved for XR system capacity (22-32%) as seen in Fig. 6. For instance, the average eMBB cell throughput decreases by roughly 12-22% depending on the XR UE's SDRs.

VI. Conclusions

This paper presents a dynamic XR-aware ICIC technique that enhances XR capacity while minimizing the eMBB performance degradation. The proposed technique identifies victim XR UEs based on their performance metrics (delay, DIR, and SINR) and coordinates with aggressor cells to temporarily mute their transmissions. This approach significantly improves victim UEs' channel quality, leading to a substantial boost in XR capacity. Extensive system-level simulations confirm the benefits of the dynamic ICIC solution, achieving a 22-32% increase in XR capacity while causing an acceptable 12-22% reduction in average eMBB cell throughput. The findings of this study provide valuable insights for network infrastructure vendors to offer XR-aware RRM/ICIC solutions. Implementing these schemes in gNB products enables operators to control the trade-off of XR and eMBB performance.

References

[1] 3GPP Technical Report 38.838 V17.0.0, "Study on XR (Extended Reality) Evaluations for NR (Release 17)," Dec., 2021.

[2] 3GPP Technical Report 38.835 V18.0.1, "Study on XR enhancements for NR (Release 18)," Apr., 2023.

[3] 3GPP Work Item Description RP-234057, "New WID: XR (eXtended Reality) for NR Phase 3," Dec., 2023.

[4] E. Chen *et al.*, "Frame-Level Integrated Transmission for Extended Reality over 5G and Beyond," in *2021 IEEE Global Communications Conference (GLOBECOM)*. IEEE, Dec., 2021, pp. 1–6.

[5] F. Hu *et al.*, "Cellular-connected wireless virtual reality: Requirements, challenges, and solutions," *IEEE Commun. Mag.*, vol. 58, no. 5, pp. 105–111, 2020.

[6] G. Minopoulos *et al.*, "Opportunities and Challenges of Tangible XR Applications for 5G Networks and Beyond," *IEEE Consumer Electronics Magazine*, Mar., 2022.

[7] P. Paymard *et al.*, "Performance of Joint XR and Best Effort eMBB Traffic in 5G-Advanced Networks," 2023. [Online]. Available: https://arxiv.org/abs/2301.08489

[8] B. Soret *et al.*, "Interference Coordination for 5G New Radio," *IEEE Wireless Communications*, vol. 25, no. 3, pp. 131–137, 2018.

[9] A. S. Hamza *et al.*, "A Survey on Inter-Cell Interference Coordination Techniques in OFDMA-Based Cellular Networks," *IEEE Communications Surveys & Tutorials*, vol. 15, no. 4, pp. 1642–1670, 2013.

[10] H. Kim *et al.*, "Dynamic TDD Systems for 5G and Beyond: A Survey of Cross-Link Interference Mitigation," *IEEE Communications Surveys & Tutorials*, vol. 22, no. 4, pp. 2315–2348, 2020.

[11] N. H. Mahmood *et al.*, "Interference Aware Inter-Cell Rank Coordination for 5G Systems," *IEEE Access*, vol. 5, pp. 2339–2350, 2017.

[12] B. Soret *et al.*, "On-Demand Power Boost and Cell Muting for High Reliability and Low Latency in 5G," in *2017 IEEE 85th Vehicular Technology Conference (VTC Spring)*, June, 2017, pp. 1–5.

[13] K. I. Pedersen *et al.*, "Dynamic Enhanced Intercell Interference Coordination for Realistic Networks," *IEEE Transactions on Vehicular Technology*, vol. 65, no. 7, pp. 5551–5562, 2016.

[14] P. Paymard *et al.*, "Optimizing Mixed Capacity of Extended Reality and Mobile Broadband Services in 5G-Advanced Networks," *IEEE Access*, vol. 11, pp. 113 324–113 338, 2023.

[15] ——, "Enhanced CQI to Boost the Performance of 5G-Advanced XR With Code Block Group Transmissions," *IEEE Transactions on Vehicular Technology*, pp. 1–13, 2023.

[16] ——, "Enhanced Link Adaptation for Extended Reality Code Block Group based HARQ Transmissions," in *2022 IEEE Globecom Workshops (GC Wkshps)*, 2022, pp. 711–716.

[17] P. Ameigeiras *et al.*, "Performance of the M-LWDF scheduling algorithm for streaming services in HSDPA," in *IEEE 60th Vehicular Technology Conference (VTC)-Fall. 2004*, vol. 2, 2004, pp. 999–1003 Vol. 2.

[18] V. Fernandez-Lopez *et al.*, "Effects of Interference Mitigation and Scheduling on Dense Small Cell Networks," in *2014 IEEE 80th Vehicular Technology Conference (VTC2014-Fall)*, Sep., 2014, pp. 1–5.

[19] 3GPP Technical Specification 38.423 V18.0.0, "NG-RAN; Xn application protocol (XnAP)(Release 18)," Dec., 2023.

[20] P. Paymard *et al.*, "PDU-set Scheduling Algorithm for XR Traffic in Multi-Service 5G-Advanced Networks," *Accepted for publication in 2024 IEEE International Conference on Communications (ICC)*, June, 2024. [Online]. Available: https://arxiv.org/abs/2311.08969

[21] N. Varshney *et al.*, "Link-Level Abstraction of IEEE 802.11ay based on Quasi-Deterministic Channel Model from Measurements," in *2020 IEEE 92nd Veh. Technol. Conf. (VTC2020-Fall)*, Nov., 2020, pp. 1–7.

[22] K. Pedersen *et al.*, "A Tutorial on Radio System-Level Simulations With Emphasis on 3GPP 5G-Advanced and Beyond," *IEEE Communications Surveys & Tutorials*, pp. 1–1, 2024.